

Stationary states of a spherical Minority Game with ergodicity breaking

Tobias Gallat^{†‡}, David Sherrington[‡]

[†] International Center for Theoretical Physics, Strada Costiera 11, 34014 Trieste, Italy and CNR-INFM, Trieste-SISSA Unit, V. Beirut 2-4, 34014 Trieste, Italy

[‡] The Rudolf Peierls Centre for Theoretical Physics, Department of Physics, University of Oxford, 1 Keble Road, Oxford OX1 3NP, UK

Abstract. Using generating functional and replica techniques, respectively, we study the dynamics and statics of a spherical Minority Game (MG), which in contrast with a spherical MG previously presented in [1] displays a phase with broken ergodicity and dependence of the macroscopic stationary state on initial conditions. The model thus bears more similarity with the original MG. Still, all order parameters including the volatility can be computed in the non-ergodic phases without making any approximations. We also study the effects of market impact correction on the phase diagram. Finally we discuss a continuous-time version of the model as well as the differences between on-line and batch update rules. Our analytical results are confirmed convincingly by comparison with numerical simulations. In an appendix we extend the analysis of [1] to a model with general time-step, and compare the dynamics and statics of the two spherical models.

PACS numbers: 02.50.Le, 87.23.Ge, 05.70.Ln, 64.60.Ht

E-mail: galla@ictp.trieste.it, sherr@thphys.ox.ac.uk

1. Introduction

The introduction of continuous versions of spin systems with discrete degrees of freedom is common in statistical mechanics and has led to a better analytical understanding of many basic features displayed by various spin models. The appeal of continuous models lies in the fact that calculations are simplified considerably compared to their counterparts with discrete Ising spins, so that in many cases a full analytical solution of the models with continuous spins becomes possible. The general procedure is to replace the discrete Ising-like variables $s_i \in \{-1, 1\}$ of a given spin system by continuous variables $\phi_i \in \mathbb{R}$. If we assume that the system is composed of N such spins ($i = 1, \dots, N$), then often a so-called spherical constraint is imposed on all possible configurations contributing to the partition function: $\sum_i \phi_i^2 = N$. While the partition function of a system with Ising spins is a sum over configurations corresponding to the corners of an N -dimensional hypercube, this sum is effectively replaced by an integral over the surface of the sphere running through these corners. The hope is

that the simplified, spherical model still captures the relevant physical features of the original model and allows to shed some light on its basic phenomenology despite the simplification.

The first example of a spherical model is the one of a ferromagnet introduced more than fifty years ago by Berlin and Kac [2]. It is the continuous analogue of the Ising model, and can be solved exactly in all dimensions, and exhibits a phase transition corresponding to the onset of spontaneous magnetization. Spherical counterparts of the Sherrington-Kirkpatrick model have played and are playing an important role in the study of spin-glasses, and similar mean-field models with higher-order couplings between the continuous spins are able to capture some of the essential features of structural glasses. Recently a spherical version of the Hopfield model of neural networks has been considered in [3], and a spherical Minority Game (MG) was introduced in [1]. The present work is a continuation of [1], and we will here devise an alternative way of formulating a spherical limit of the MG.

The Minority Game [4] is a simplified model of interacting traders in a financial market and has become one of the most studied models in the econophysics community [5, 6, 7]. From the point of view of statistical mechanics the MG is a fully connected mean-field disordered system. Analytical progress can therefore be made using the standard tools of equilibrium and non-equilibrium statistical mechanics, such as replica theory and generating functionals. With these methods an ergodic/non-ergodic phase transition has been identified in the MG, and static order parameters in the ergodic regime computed within a replica-symmetric ansatz agree with numerical simulations. The dynamical approach furthermore allows one to formulate a self-consistent theory for all regimes of the game in terms of a single effective-agent process [6]. This effective problem is fully equivalent to the coupled multi-agent dynamics of the MG in the thermodynamic limit and analytical results for persistent order parameters in the ergodic phase can be obtained from this effective process in agreement with the results derived from the statics. These solutions are now regarded as exact. A proper understanding of the non-ergodic phase is however still awaited. Moreover, for the conventional MG the so-called ‘market volatility’ (one of the MG’s main observables) cannot be computed exactly and results are here restricted to approximations even in the ergodic phase.

In [1] a spherical version of the MG was presented, offering the possibility of a more complete solution. The non-linear dynamics of the conventional MG was replaced by effectively linear equations, resulting in an exactly solvable harmonic model. Despite the simplicity of the update rules this model was shown to exhibit a non-trivial phase diagram with three distinct phases and different types of phase transitions. All stationary observables (including the volatility) can here be computed in all phases without making any approximations. The model discussed in [1] however has only limited similarity compared to the original MG. For example the behaviour of the volatility turns out to be quite different in both models, and crucially the spherical model presented in [1] does not exhibit any phases in which the macroscopic dynamics and the resulting stationary states depend on initial conditions. This is in sharp contrast

with the original MG, in which initial conditions have been found to be relevant in the non-ergodic phase and where the resulting memory effects have to a great part been responsible for the interest of statistical physicists in the MG.

In this paper we will therefore consider a spherical limit of the MG, which is different from the route taken in [1], leading to a model with a phenomenology closer to that of the original MG. In particular the model studied in this paper displays non-ergodicity and memory effects. Nevertheless it is exactly solvable, and we are able to derive expressions for the volatility in the ergodic regime without making any approximations. We here choose to concentrate on the stationary states of the model and do not address its transient dynamics. While we present some numerical results for the non-ergodic phase a more detailed analysis would here require a full solution for the transient dynamics in order to keep track of the effects of the state from which the dynamics is started. This is beyond the scope of the present paper but might be considered in later studies.

The remainder of this paper is organized as follows: In section 2 we introduce the model, section 3 is concerned with the study of the dynamics, and in section 4 we discuss the resulting phase diagram. The statics are considered in section 5. Finally we present a comparison of the batch model with its continuous time limit (section 6) and with its on-line counterpart (section 7), before we draw conclusions in the final section. The appendix provides a discussion of some aspects of the earlier spherical MG not addressed in [1] as well as a comparison of the two spherical models.

2. Model Definitions

Before turning to spherical versions of the MG, it will be useful to briefly summarise the definition of the MG in its conventional setup. The MG describes an ensemble of N agents, whom we shall label by Roman indices. At each round t of the game, each agent i takes a binary trading decision $b_i(t) \in \{-1, 1\}$ in response to the observation of a publicly available piece of information $I_{\mu(t)}$. The aim of each agent is then to make the opposite choice to the majority of agents. In this paper we will assume that $\mu(t)$ is chosen randomly and independently from a flat distribution over the set $\mu(t) \in \{1, \dots, \alpha N\}$ at each time-step. This is the so-called MG with random external information. The key control parameter of the model is the ratio α of the number of possible values of the information over the number of players. We will only consider the case in which α does not scale with N , i.e. $\alpha = \mathcal{O}(N^0)$. The (re-scaled) total market at time-step t is then defined as $A(t) = N^{-1/2} \sum_i b_i(t)$. To take trading decisions each agent i has two strategies $\mathbf{R}_{ia} = (R_{ia}^1, \dots, R_{ia}^{\alpha N}) \in \{-1, 1\}^{\alpha N}$ at his or her disposal, with $a = \pm 1$ [‡]. These effectively act as look-up tables mapping the values μ of the external information onto a trading decision R_{ia}^μ . If agent i decides to use strategy $s_i(t) \in \{-1, 1\}$ in round t his or her bid at this stage will be $R_{is_i(t)}^{\mu(t)}$. In this paper we will assume that all strategies are drawn randomly and independently before the start of the game and

[‡] The MG problem can be generalised to include more strategies per agent, but here we concentrate on this technically simpler but still representative case.

that the components $\{R_{ia}^\mu\}$ take the values ± 1 with equal probability; the strategies then remain fixed, they represent the quenched disorder of the problem. In order to decide which of their two strategies to use each agent keeps track of the performance of both of his or her strategies by assigning virtual scores $p_{ia}(t)$ based on what would have happened had he or she always played that particular strategy. These scores are updated according to

$$p_{ia}(t+1) = p_{ia}(t) - \frac{R_{ia}^{\mu(t)}}{\sqrt{N}} \left[A(t) - \frac{\kappa}{\sqrt{N}} (R_{is_i(t)}^{\mu(t)} - R_{ia}^{\mu(t)}) \right]. \quad (1)$$

Note that the minus sign in front of the square bracket ensures that strategies which would have produced a minority decision are rewarded. The term proportional to κ takes into account a correction of the impact of trader i 's action on the total market bit, and can be seen as an analogue of an Onsager reaction term; see [8, 9] for details. The additional model parameter κ can take values $0 \leq \kappa \leq 1$, with $\kappa = 0$ corresponding to the absence of impact-correction and $\kappa = 1$ to so-called 'sophisticated agents' or 'full impact correction'§. In the conventional MG each player then uses the strategy with the highest score, i.e. $s_i(t) = \arg \max_a p_{ia}(t)$. In order to determine which of the two strategies to use, it is sufficient to consider the score difference $q_i(t) = \frac{1}{2}[p_{i,1}(t) - p_{i,-1}(t)]$, then one has $s_i(t) = \text{sgn}[q_i(t)]$, and upon introduction of $\boldsymbol{\omega}_i = \frac{1}{2}[\mathbf{R}_{i,1} + \mathbf{R}_{i,-1}]$ and $\boldsymbol{\xi}_i = \frac{1}{2}[\mathbf{R}_{i,1} - \mathbf{R}_{i,-1}]$ the bid of player i at time t may be written as $b_i(t) = \omega_i^{\mu(t)} + s_i(t)\xi_i^{\mu(t)}$. The evolution of the $\{q_i\}$ is then given by

$$q_i(t+1) = q_i(t) - \frac{\xi_i^{\mu(t)}}{\sqrt{N}} \left[\Omega^{\mu(t)} + N^{-1/2} \sum_j \xi_j^{\mu(t)} s_j(t) - \frac{\kappa}{\sqrt{N}} \xi_i^{\mu(t)} s_i(t) \right], \quad (2)$$

where $\boldsymbol{\Omega} = N^{-1/2} \sum_j \boldsymbol{\omega}_j$. This defines the so-called 'on-line' MG. Alternatively one may consider models in which the agents update the $\{q_i(t)\}$ only every $\mathcal{O}(N)$ time-steps. This leads to an effective average over all possible values of the external information and results in the so-called batch MG [10]:

$$q_i(t+1) = q_i(t) - h_i - \sum_j J_{ij} s_j(t) + \kappa \alpha s_i(t). \quad (3)$$

Here $J_{ij} = 2N^{-1} \boldsymbol{\xi}_i \cdot \boldsymbol{\xi}_j$ and $h_i = 2N^{-1} \boldsymbol{\xi}_i \cdot \boldsymbol{\Omega}$.

These batch and on-line update rules provide suitable starting points for the introduction of spherical versions of the MG. In [1] Eq. (3) was replaced by (only the case $\kappa = 0$ was considered there)

$$[1 + \lambda(t+1)]q_i(t+1) = q_i(t) - h_i - \sum_j J_{ij} q_j(t) \quad (4)$$

and the $\{\lambda(t)\}$ were chosen to impose a global spherical constraint $\sum_i q_i(t)^2 = Nr^2$ for all t . Although inspired by the spherical limits sometimes imposed on models of

§ In the conventional MG the impact-correction term was found to have crucial consequences for the properties of the model. The game without impact correction shows an ergodic/non-ergodic phase transition, but no replica-symmetry breaking. In the game with impact correction ($\kappa > 0$) a de Almeida-Thouless transition of a different type, along with the onset of long-term memory at finite integrated response, is found [8, 9].

magnetic systems where Ising variables $s_i = \pm 1$ are replaced by continuous spins ϕ_i subject only to the same global constraint $\sum_{i=1}^N \phi_i^2 = N = \sum_{i=1}^N s_i^2$, without the local constraint $s_i^2 = 1$, the situation in the earlier spherical MG model is at variance with the original MG in that the latter does not obey $q_i^2 = \text{constant}$. Rather it is $s_i = \text{sgn}[q_i]$ which obeys $s_i^2 = 1$ for all i in the MG. In the present paper we will therefore consider the replacement $s_i(t) \rightarrow \phi_i(t)$ with continuous variables $\{\phi_i(t)\}$, and will impose a spherical constraint only on the $\{\phi_i\}$, but not on the $\{q_i\}$. Specifically, we will consider a batch model defined by

$$q_i(t+1) = q_i(t) - h_i - \sum_j J_{ij} \phi_j(t) + \kappa \alpha \phi_i(t), \quad (5)$$

where

$$\phi_i(t) = \frac{q_i(t)}{\lambda(t)}, \quad \lambda(t) = \left[N^{-1} \sum_i q_i(t)^2 \right]^{1/2}, \quad (6)$$

so that the $\{\phi_i(t)\}$ obey the spherical constraint $\sum_i \phi_i(t)^2 = N$ for all t , in analogy to the $\{s_i(t) = \pm 1\}$ in the original MG. The corresponding on-line model is defined by

$$q_i(t+1) = q_i(t) - \frac{\xi_i^{\mu(t)}}{\sqrt{N}} \left[\Omega^{\mu(t)} + N^{-1/2} \sum_j \xi_j^{\mu(t)} \phi_j(t) - \frac{\kappa}{\sqrt{N}} \xi_i^{\mu(t)} \phi_i(t) \right], \quad (7)$$

where we again impose (6). In principle more general dependencies of the $\{\phi_i\}$ on the $\{q_i\}$ could be considered. We here chose the ϕ_i to be proportional to the q_i to guarantee the solvability of the resulting harmonic model. Also we assume $\lambda(t) > 0$, i.e. $\phi_i(t)$ is taken to have the same sign as $q_i(t)$.

An interpretation of spherical updates rules in terms of the decision making of the agents was given in [1]: while the agents in conventional MGs have at each time-step to decide which of their two strategies they wish to use, they are playing linear combinations of their strategies in the spherical case. The two spherical limits differ in the way this linear combination is determined. Moreover the models defined by Eqs. (5) and (7) allow for runaway solutions $q_i(t) \rightarrow \pm\infty$ (potentially resulting in an asymptotically divergent normalization factor $\lambda(t)$), which are suppressed by the spherical constraint on the $\{q_i(t)\}$ in the earlier spherical model||.

Let us finally, in this section, introduce one of the key observables in MGs, the so-called volatility σ^2 . It describes the variance of the total re-scaled market bid A , and can be defined as the following long-time average:

$$\sigma^2 = \lim_{\tau \rightarrow \infty} \tau^{-1} \sum_{t \leq \tau} A(t)^2 \quad (8)$$

in on-line models. In batch games an additional average over the external information is to be performed and one has

$$\sigma^2 = \lim_{\tau \rightarrow \infty} (\alpha N \tau)^{-1} \sum_{t \leq \tau} \sum_{\mu=1}^{\alpha N} (A^\mu(t))^2, \quad (9)$$

|| Such runaway solutions, in which the $|q_i(t)|$ increase linearly with t , are a standard feature of the conventional MG, corresponding to agents described as ‘frozen’ [5, 6].

where $A^\mu(t) = \Omega^\mu + N^{-1/2} \sum_i \xi_i^\mu \phi_i(t)$; for further details see also [10, 1, 11]. Note that stochastic trading with the $\{\phi_i(t)\}$ taken randomly and independently at any time step t from the spherical surface $\sum_i \phi_i^2(t) = N$ would result in $\sigma^2 = 1$. This is referred to as the random trading limit.

3. Generating functional analysis

3.1. Effective single-agent process and macroscopic dynamics

We will now proceed by studying the dynamics of the present spherical model using generating functionals. This approach is now standard in the context of MGs, and leads to a self-consistent problem for the correlation and response functions formulated in terms of a single effective trader equation. Due to the similarity of the present model with the conventional batch MG and the spherical model presented in [1] we can obtain the single effective agent equation corresponding to the process (5,6) by some minor modifications of the results of [10, 1]. One finds

$$q(t+1) = q(t) + \theta(t) - \alpha \sum_{t' \leq t} (\mathbf{I} + G)_{tt'}^{-1} \phi(t') + \alpha \kappa \phi(t) + \sqrt{\alpha} \eta(t), \quad (10)$$

where $\phi(t) = \frac{q(t)}{\lambda(t)}$.

Here $\theta(t)$ is an external perturbation field introduced to generate response functions and $\eta(t)$ is a zero-average Gaussian noise with temporal correlations characterized by the following covariance matrix (with $D_{tt'} = 1 + C_{tt'}$ for all t, t' , and \mathbf{I} the identity matrix):

$$\Gamma_{tt'} = \langle \eta(t) \eta(t') \rangle_* = [(\mathbf{I} + G)^{-1} D (\mathbf{I} + G^T)^{-1}]_{tt'}. \quad (11)$$

The matrices \mathbf{C} and \mathbf{G} and the normalization factors $\boldsymbol{\lambda} = \{\lambda(t)\}$ are the dynamical order parameters of the problem, to be determined self-consistently upon solving

$$C_{tt'} = \langle \phi(t) \phi(t') \rangle_*, \quad G_{tt'} = \frac{\partial}{\partial \theta(t')} \langle \phi(t) \rangle_*, \quad C_{tt} = 1 \quad \forall t, t'. \quad (12)$$

The brackets $\langle \dots \rangle_*$ in (11, 12) refer to averages over realizations of the process (10), i.e. over the noise $\{\eta(t)\}$. The resulting self-consistent problem for $\{\mathbf{C}, \mathbf{G}, \boldsymbol{\lambda}\}$ is equivalent to the original batch process in the thermodynamic limit $N \rightarrow \infty$. In particular, the physical meaning of the matrices \mathbf{C} and \mathbf{G} is given by

$$C_{tt'} = \lim_{N \rightarrow \infty} N^{-1} \sum_i \overline{\langle \phi_i(t) \phi_i(t') \rangle}, \quad (13)$$

$$G_{tt'} = \lim_{N \rightarrow \infty} N^{-1} \sum_i \frac{\partial}{\partial \theta(t')} \overline{\langle \phi_i(t) \rangle}, \quad (14)$$

where $\overline{\dots}$ denotes an average over the disorder, i.e. over the space of all strategy assignments, and $\langle \dots \rangle$ stands for an average over possibly random initial conditions (and/or decision noise in case stochastic trading is considered [12]). As usual the single effective agent process is non-Markovian and contains coloured Gaussian noise.

Similar to [1] it is possible to convert the system (10, 11, 12) into a pair of explicit iterative equations for \mathbf{C} and \mathbf{G} and $\boldsymbol{\lambda}$; note that due to the non-linearity

in $s_i(t) = \text{sgn}[q_i(t)]$ such a conversion is in general not possible for conventional MGs. We find

$$\begin{aligned} \lambda(t+1)C_{t+1,t'} - (\lambda(t) + \alpha\kappa)C_{tt'} &= \alpha[(\mathbf{I} + G)^{-1}D(\mathbf{I} + G^T)^{-1}G^T]_{tt'} \\ &\quad - \alpha[(\mathbf{I} + G)^{-1}C]_{tt'}, \end{aligned} \quad (15)$$

$$\lambda(t+1)G_{t+1,t'} - (\lambda(t) + \alpha\kappa)G_{tt'} = -\alpha[(\mathbf{I} + G)^{-1}G]_{tt'} + \delta_{tt'}. \quad (16)$$

Eqs. (15, 16) have to be solved subject to the constraint $C_{tt} = 1$ for all $t \geq 0$. Furthermore one finds as in [10] for $N \rightarrow \infty$ that the rescaled disorder-averaged total bid $\overline{\langle A(t) \rangle}$ is zero for all times, and that the disorder-averaged volatility is asymptotically given by the diagonal elements of the covariance matrix of the single-agent noise:

$$\sigma^2 = \frac{1}{2} \lim_{\tau \rightarrow \infty} \tau^{-1} \sum_{t \leq \tau} [(\mathbf{I} + G)^{-1}D(\mathbf{I} + G^T)^{-1}]_{tt}. \quad (17)$$

Already at this stage one may notice that Eqs. (15, 16) allow in principle for non-ergodic behaviour. The value $\lambda(t=0) = \left[\lim_{N \rightarrow \infty} N^{-1} \sum_{i=1}^N \overline{\langle q_i(0)^2 \rangle} \right]^{1/2}$ is not fixed by the dynamics, but is set by the initial conditions from which the dynamics is started. The type of stationary state reached asymptotically may hence depend on the starting point, similarly to what is observed in conventional MGs, and at variance with the behaviour of the spherical model defined by (4), where the macroscopic dynamics at all times is fully fixed by the model parameter r . We will discuss the effects of different starts $|q_i(0)| = q_0$ for all i with varying bias q_0 below.

3.2. Time-translation invariant ergodic states

We will consider the system long after any initial equilibration and focus on time-translation invariant (TTI) solutions of the coupled equations (15, 16) of the form

$$\lim_{t \rightarrow \infty} C_{t+\tau,t} = C(\tau), \quad \lim_{t \rightarrow \infty} G_{t+\tau,t} = G(\tau). \quad (18)$$

In addition we make the standard assumptions of finite integrated response and weak long-term memory:

$$\chi \equiv \lim_{t \rightarrow \infty} \sum_{\tau \leq t} G(\tau) < \infty, \quad \lim_{t \rightarrow \infty} G_{t,t'} = 0 \quad \forall t' \text{ finite.} \quad (19)$$

The order parameter λ comes out as a function of the form $\lambda(t) = \lambda_0 + \lambda_1 t$ asymptotically in simulations, with λ_0 and λ_1 constants. As it turns out we will find two distinct phases with the above properties:

- (i) an oscillatory phase in which $\lim_{t \rightarrow \infty} \lambda(t)$ remains finite, i.e. $\lambda_1 = 0$ and
- (ii) a frozen phase in which $\lambda(t)$ grows linearly in time asymptotically, i.e. $\lambda_1 > 0$.

We will refer to these phases as ‘bounded’ and ‘unbounded’ in the following, and will discuss them separately ¶.

¶ One may argue whether a phase with a linearly growing order parameter $\lambda(t)$ qualifies as time-translation invariant. Note however that the stationary ergodic states of the standard MG also contain runaway solutions of the type $q_i(t) \rightarrow \pm\infty$, so-called frozen agents, so that $N^{-1} \sum_i q_i(t)^2$ diverges in time. In the unbounded phase we find that $\lambda(t)/t$ is the stationary quantity asymptotically.

3.2.1. Bounded oscillatory states ($\lambda_1 = 0$) We here consider $\lambda(t) \equiv \lambda_0$. Given our TTI ansatz (18) all matrices in (15, 16) become Toeplitz matrices in the stationary state, and hence they commute. It is then furthermore convenient to introduce Fourier transforms of the correlation and response functions according to

$$C(\tau) = \int_{-\pi}^{\pi} \frac{d\omega}{2\pi} e^{i\omega\tau} \tilde{C}(\omega), \quad \tilde{C}(\omega) = \sum_{\tau} e^{-i\omega\tau} C(\tau) \quad (20)$$

and similarly for G . Now upon setting $\lambda(t) \equiv \lambda_0$ in the stationary state, Eqs. (15, 16) translate into

$$[\lambda_0(e^{i\omega} - 1) - \alpha\kappa] \tilde{C}(\omega) = \frac{\alpha\tilde{D}(\omega)\tilde{G}(\omega)^*}{|1 + \tilde{G}(\omega)|^2} - \frac{\alpha\tilde{C}(\omega)}{1 + \tilde{G}(\omega)}, \quad (21)$$

$$[\lambda_0(e^{i\omega} - 1) - \alpha\kappa] \tilde{G}(\omega) = 1 - \frac{\alpha\tilde{G}(\omega)}{1 + \tilde{G}(\omega)}. \quad (22)$$

Here $\tilde{G}(\omega)^*$ denotes the complex conjugate of $\tilde{G}(\omega)$. Using $\tilde{D}(\omega) = \tilde{C}(\omega) + 2\pi\delta(\omega)$ as well as the definition of the integrated response $\chi = \sum_{\tau} G(\tau) = \tilde{G}(0)$ we may write (21) as

$$\left[\{\lambda_0(e^{i\omega} - 1) - \alpha\kappa\} |1 + \tilde{G}(\omega)|^2 + \alpha \right] \tilde{C}(\omega) = 2\pi\alpha\chi\delta(\omega). \quad (23)$$

From this equation it follows immediately that $\tilde{C}(\omega)$ can be non-zero for any $\omega \neq 0$ only if $e^{i\omega}$ is real, i.e. for $\omega = \pi$. Consequently $\tilde{C}(\omega)$ must be of the form $\tilde{C}(\omega) = 2\pi[c_0\delta(\omega) + c_1\delta(\omega - \pi)]$. Equivalently we may write

$$C(\tau) = c_0 + c_1(-1)^{\tau}. \quad (24)$$

Note that we always have $c_0 + c_1 = 1$ due to the spherical constraint $C(\tau = 0) = 1$. Inserting this ansatz into (21,22) and setting $\omega = 0$ then leads to the following relations

$$\alpha\kappa c_0 = -\frac{\alpha(1 + c_0)\chi}{(1 + \chi)^2} + \alpha\frac{c_0}{1 + \chi}, \quad \alpha\kappa\chi = -\frac{1 + (1 - \alpha)\chi}{1 + \chi}. \quad (25)$$

After some algebra the physically relevant solutions are identified as

$$c_0 = \left[\left(\frac{1 + (1 - \kappa)\alpha + \sqrt{[1 + (1 - \kappa)\alpha]^2 - 4\alpha}}{2\sqrt{\alpha}} \right)^2 - 1 \right]^{-1}, \quad (26)$$

$$\chi = [\sqrt{\alpha}\sqrt{1 + 1/c_0} - 1]^{-1}. \quad (27)$$

This determines c_0 and χ as functions of α and κ , and simplifies to $c_0 = \chi = \frac{1}{\alpha-1}$ for $\kappa = 0$. The expression for c_0 implies that a fully frozen solution ($c_0 = 1$) can be realised only at the point given by

$$\alpha_{c1}(\kappa) = \frac{5 + 4\kappa + 3\sqrt{1 + 8\kappa}}{4(1 - \kappa)^2}. \quad (28)$$

This describes a line in the (α, κ) -plane, so that there can be no frozen TTI phases with finite integrated response and with a finite value of $\lambda_0 = \lim_{t \rightarrow \infty} t^{-1} \sum_{\tau \leq t} \lambda(\tau)$. We can therefore focus on solutions with $c_0 < 1$. These are solutions in which oscillations of

the correlation function persist, so that the oscillation amplitude $c_1 = 1 - c_0$ is strictly positive. Setting $\omega = \pi$ in (21,22) gives

$$((-2\lambda_0 - \alpha\kappa)(1 + \chi')^2 + \alpha)(1 - c_0) = 0, \quad (29)$$

$$(-2\lambda_0 - \alpha\kappa)\chi' = 1 - \frac{\alpha\chi'}{1 + \chi'}. \quad (30)$$

Here $\chi' = \sum_{\tau} (-1)^{\tau} G(\tau) = \tilde{G}(\pi)$ measures the response of the system to persistent oscillatory perturbations. Looking only for oscillatory solutions ($c_1 > 0$, $c_0 < 1$) we must require $(2\lambda_0 + \alpha\kappa)(1 + \chi')^2 = \alpha$ in this regime. Using this and (30) we find the following solutions valid for $\alpha > \alpha_{c1}(\kappa)$:

$$\lambda_0 = \frac{1}{2}[\alpha + 1 + 2\sqrt{\alpha} - \alpha\kappa], \quad \chi' = -\frac{1}{1 + \sqrt{\alpha}}. \quad (31)$$

The persistent order parameters in the ergodic bounded oscillatory state are thus fully described by Eqs. (27, 26, 31). The consistency of this ansatz breaks down whenever $\chi \rightarrow \infty$ or $c_0 \rightarrow 1$. From (28) one observes that $c_0 \rightarrow 1$ at a value of $\alpha = \alpha_{c1} \geq 2$, whereas (27) dictates that χ remains finite for all $\alpha \geq 1$ for any fixed value of $\kappa \geq 0$. Hence we conclude that the oscillation amplitude vanishes before anomalous response sets in as α is lowered at a fixed value of κ . We thus expect a transition to a frozen state at finite integrated response.

Finally, using the fact that $C(\tau) = c_0 + (1 - c_0)(-1)^{\tau}$ the volatility in the stationary state can be obtained from Eq. (17) as

$$\sigma^2 = \frac{1}{2} \left[(\mathbf{I} + G)^{-1} D (\mathbf{I} + G^T)^{-1} \right] (0) = \frac{1}{2} \left[\frac{1 + c_0}{(1 + \chi)^2} + \frac{1 - c_0}{(1 + \chi')^2} \right]. \quad (32)$$

Note that this is an exact result, with no approximations made at any stage.

3.2.2. Unbounded frozen states ($\lambda_1 > 0$) A second type of time-translation invariant solutions can be found upon making the ansatz

$$C_{t,t'} \equiv 1, \quad G_{t,t'} = G(t - t') \quad \forall t, t', \quad (33)$$

but giving up the assumption that $\lambda(t) = \lambda_0$ be constant. Instead, these solutions correspond to a fully frozen state, and we find in numerical simulations that

$$\lambda(t) = \lambda_0 + \lambda_1 t \quad (34)$$

for a constant $\lambda_1 > 0$ (yet to be determined) and that the $q_i(t)$ take the form $q_i(t) = v_i t$. In order to compute the persistent order parameters, it here turns out to be convenient to work with the effective process rather than with the closed equations for C and G . Upon making the ansatz $q(t) = vt$ for solutions of the single-effective agent process, and assuming that $\theta(t) \equiv \theta$ is a persistent perturbation one performs an average of the effective process (10) over the time t (a similar time-averaging procedure for the effective process of the conventional batch MG is discussed in [10]) and obtains

$$v = \theta - \frac{\alpha v}{\lambda_1(1 + \chi)} + \frac{\alpha\kappa v}{\lambda_1} + \sqrt{\alpha\bar{\eta}}. \quad (35)$$

Here $\bar{\eta} = \lim_{T \rightarrow \infty} T^{-1} \sum_{t \leq T} \eta(t)$ is a static Gaussian variable of zero average and with variance $\langle \bar{\eta}^2 \rangle_{\bar{\eta}} = (1 + c_0)/(1 + \chi)^2$ (with $c_0 = 1$ in the frozen state under investigation). The only purpose of θ is to generate response functions, and noting that derivatives with respect to θ can (up to a factor $\sqrt{\alpha}$) be replaced by derivatives with respect to $\bar{\eta}$ we may set $\theta = 0$ and write

$$v = \frac{\sqrt{\alpha} \bar{\eta}}{1 + \frac{\alpha}{\lambda_1} \left(\frac{1}{1+\chi} - \kappa \right)}. \quad (36)$$

Self-consistency then demands

$$\lambda_1 = \sqrt{\langle v^2 \rangle_{\bar{\eta}}}, \quad \chi = \frac{1}{\lambda_1 \sqrt{\alpha}} \left\langle \frac{\partial v}{\partial \bar{\eta}} \right\rangle_{\bar{\eta}}. \quad (37)$$

Using (36) these relations are given by

$$\lambda_1 = \frac{\sqrt{\alpha}}{1 + \frac{\alpha}{\lambda_1} \left(\frac{1}{1+\chi} - \kappa \right)} \frac{\sqrt{2}}{(1 + \chi)}, \quad \chi = \frac{1}{\lambda_1 \left(1 + \frac{\alpha}{\lambda_1} \left(\frac{1}{1+\chi} - \kappa \right) \right)}, \quad (38)$$

and the solutions are found to be

$$\lambda_1 = -1 - \alpha + \frac{3\sqrt{\alpha}}{\sqrt{2}} + \alpha\kappa, \quad \chi = \frac{1}{\sqrt{2\alpha} - 1}. \quad (39)$$

In particular this means that the assumption of finite integrated response χ breaks down at $\alpha = \alpha_{c2} = 1/2$ so that we expect a transition to a non-ergodic phase. Note that this happens irrespective of the value of κ , in particular we could not find any signs of memory onset at finite χ in the case $\kappa > 0$, as it is observed for the conventional MG with impact correction [9]⁺.

The volatility in the frozen ergodic phase is obtained by inserting the above expression for χ into (32) (with $c_0 = 1$), and one finds

$$\sigma^2 = \frac{1}{2} \left[\sqrt{2} - \frac{1}{\sqrt{\alpha}} \right]^2. \quad (40)$$

This expression is exact and valid in the interval $\alpha \in [\alpha_{c2} = 1/2, \alpha_{c1}(\kappa)]$ for any fixed value of κ . The zeroes of $\lambda_1 = \lambda_1(\alpha)$ are found as:

$$\alpha = \frac{5 + 4\kappa \pm 3\sqrt{1 + 8\kappa}}{4(1 - \kappa)^2}. \quad (41)$$

While the upper value agrees with α_{c1} marking the boundary between the frozen and oscillatory phases with finite integrated response, we find that the lower zero of λ_1 has no relevance for $\kappa > 0$ as it occurs at a lower value of α than the onset of anomalous response at $\alpha_{c2} = 1/2$.

We have tested our theoretical predictions for the order parameters in the ergodic states against direct numerical simulations of the batch process. Results for the game

⁺ We have performed a calculation along the lines of [9], adapted to the present model, and could not observe any continuous onset of long-term memory. Also our simulations show near perfect agreement with the ergodic theory for $\kappa > 0$ so that we have no reason to suspect the breakdown of the assumption of weak long-term memory.

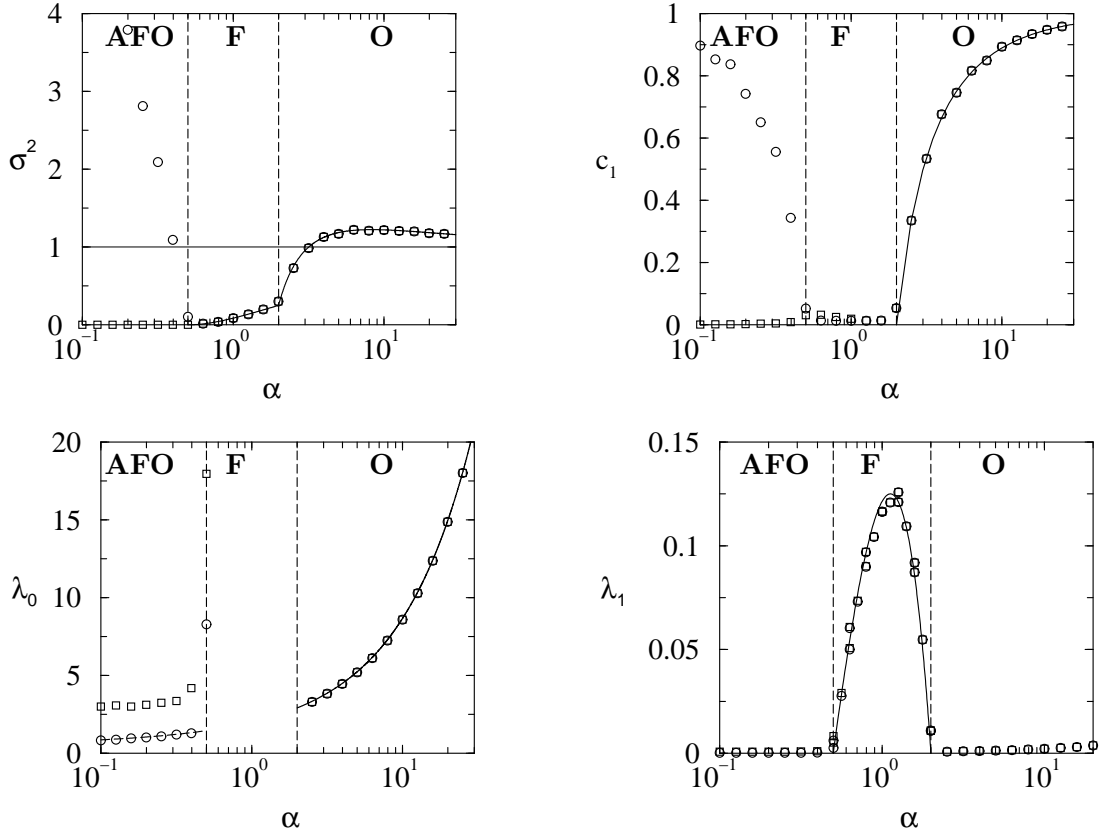


Figure 1. Volatility σ^2 , oscillation amplitude $c_1 = 1 - c_0$, and order parameters λ_0 and λ_1 for the game without impact correction ($\kappa = 0$) for different initial conditions. Markers are from simulations with $q_0 = 0.01$ (circles) and $q_0 = 3.0$ (squares) respectively. Solid lines are the theoretical predictions in the ergodic phases (continued as a dashed line into the non-ergodic phase for λ_0). **O** labels the oscillatory phase of section 3.2.1, **F** the frozen unbounded phase (section 3.2.2) and **AFO** the phase with anomalous response, in which oscillatory and frozen states can be found (section 3.3). The vertical dashed lines mark the locations of the $O \leftrightarrow F$ and $F \leftrightarrow AFO$ transitions, $\sigma^2 = 1$ is the random trading limit. Simulations are for $N = 500$ agents, run for 2000 batch steps (additionally some runs were performed for up to 20000 steps to confirm equilibration in the non-ergodic phase). All data are averages over 10 realisations of the disorder.

without impact correction ($\kappa = 0$) are displayed in Fig. 1, while Fig. 2 is concerned with the game with impact correction ($\kappa > 0$). In both cases we find near perfect agreement between the analytical theory and simulations, deviations close to the transitions points are due to finite-size and/or finite running time artifacts. The resulting phase diagram will be discussed in more detail below.

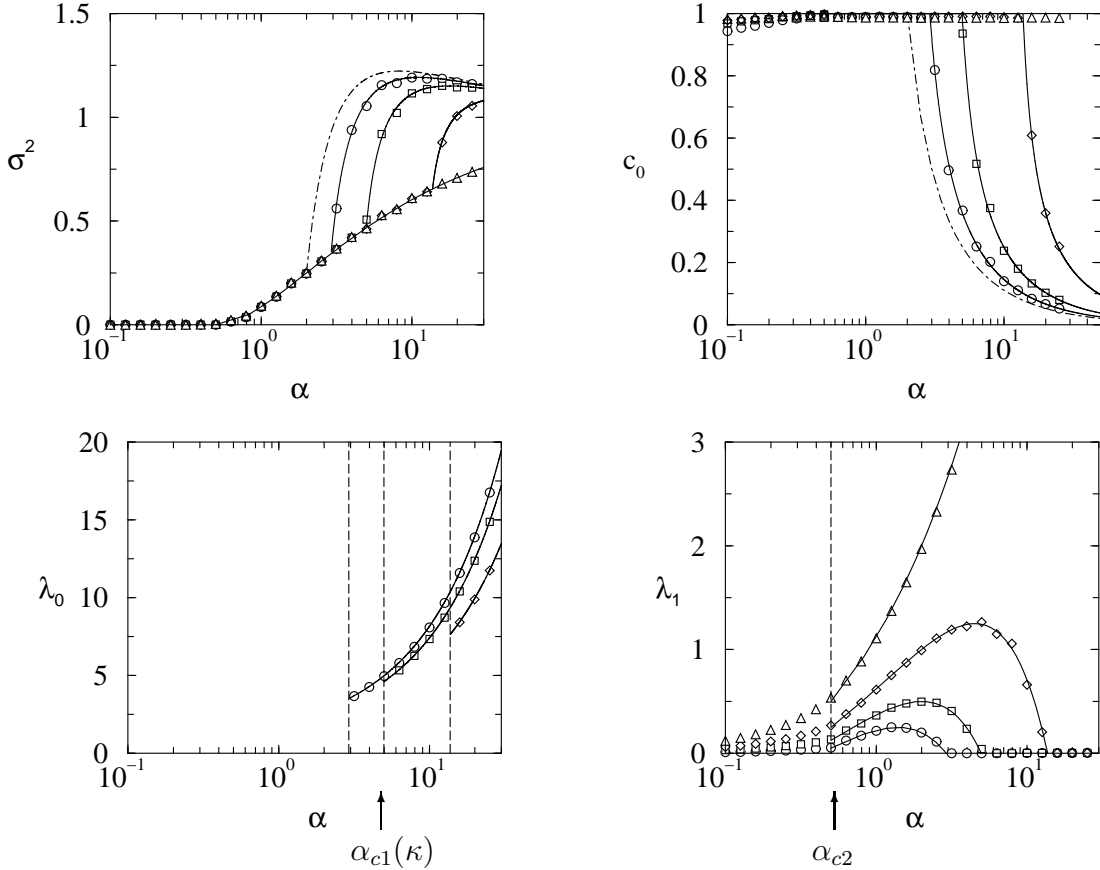


Figure 2. Volatility σ^2 , persistent correlation c_0 , order parameters λ_0 and λ_1 for the game with impact correction. Results are shown for $\kappa = 0.1$ (circles), $\kappa = 0.25$ (squares), $\kappa = 0.5$ (diamonds) and $\kappa = 1.0$ (triangles). Symbols are from simulations with $N = 500$ agents, 10 realisations, initial conditions $q_0 = 0.01$. Simulations are run for 2000 batch steps (20000 steps for the data for c_0 at $\alpha < 0.5$ in order to minimize artifacts due to incomplete equilibration). Solid lines: theory. We show the results for σ^2 and c_0 for the game at $\kappa = 0$ as dot-dashed lines in the upper two panels for comparison.

3.3. The non-ergodic phase

Throughout the non-ergodic phase one has $\chi = \infty$, and the stationary state depends on the initial conditions from which the dynamics is started. Hence, computing the asymptotic order parameters would require a full study of the intermediate transient dynamics to keep track of the influence of the starting point. This is beyond the scope of the present paper; we are here only concerned with the stationary states themselves. In numerical simulations of the non-ergodic regime of the game *without* impact-correction these states turn out to be (i) bounded and (ii) either frozen or oscillatory, so that we must assume that the ansatz $\lambda_1 = 0$ and $C(\tau) = c_0 + (1 - c_0)(-1)^\tau$ is still valid below $\alpha_{c2} = 1/2$. Setting $\chi = \infty$ in Eq. (32) (which strictly speaking has been derived only

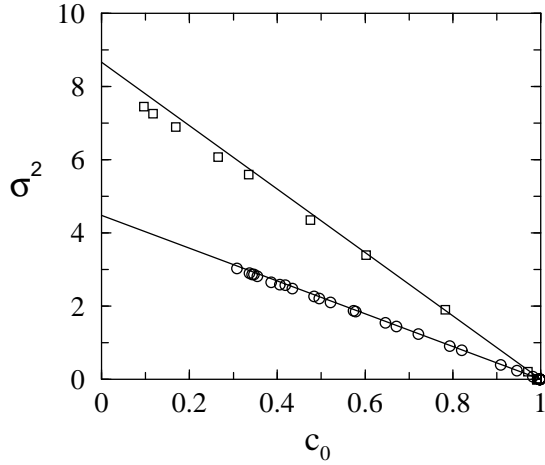


Figure 3. σ^2 vs c_0 for the game without impact correction ($\kappa = 0$) at fixed $\alpha = 0.25$ (circles) and $\alpha = 0.1$ (squares) respectively. Symbols are from simulations, every marker corresponds to a different starting point $q_i(0) = q_0$ for all i with q_0 varying from 0.01 to 2.0 in small steps. Leftmost markers correspond to $q_0 = 0.01$, rightmost symbols to frozen states resulting from high initial bias. Solid lines are Eq. (43).

under the assumptions of ergodicity and time-translation invariance) leads to

$$\sigma^2 = \frac{1}{2} \frac{1 - c_0}{(1 + \chi')^2}. \quad (42)$$

For the frozen states ($c_0 = 1$) with diverging integrated response we thus expect the volatility to vanish as confirmed in numerical simulations, see Fig. 1. Furthermore, one realises that in the derivation of (31) only the case $\omega = \pi$ in Eqs. (21,22) is used, so that χ' and λ_0 can be computed independently of c_0 and χ . We may hence conjecture that (31) still holds in the non-ergodic regime (at least in approximation). Note however that (31) can only be expected to be valid in oscillatory states as we make explicit use of the assumption $c_1 > 0$. Fig. 1 confirms that $\lambda_0 = (\alpha + 1 + 2\sqrt{\alpha})/2$ appears to describe the simulational results also in the non-ergodic regime, as long as the system is initialized at a small bias leading to an oscillatory regime. Insertion into (42) gives

$$\sigma^2 = \frac{1}{2} \frac{(1 + \sqrt{\alpha})^2}{\alpha} (1 - c_0). \quad (43)$$

As shown in Fig. 3 this relation turns out to be valid to a very good accuracy. The set of possible solutions in the non-ergodic phase thus appears to be parametrized by c_0 , with different values attained depending on initial conditions.*

* Simulations of the game without impact-correction and at fixed $\alpha < \alpha_{c2} = 1/2$ seem to indicate that oscillatory solutions are realised for initial biases q_0 smaller than some critical value $q_{0c}(\alpha)$. In this regime c_0 is an increasing function of q_0 . Starting points $q_0 > q_{0c}(\alpha)$ lead to frozen states with $c_0 = 1$ and vanishing volatility. From our simulations we cannot rule out that $q_{0c}(\alpha)$ may indeed depend on α . A similar threshold separating non-ergodic states with diverging and vanishing volatilities respectively has been identified in [10] in the limit $\alpha \rightarrow 0$ of the conventional MG.

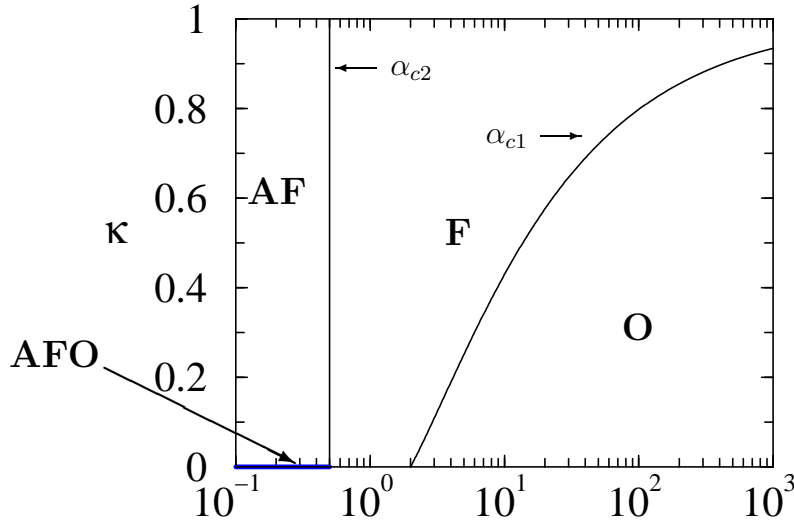


Figure 4. Phase diagram in the (α, κ) -plane. **O** marks the ergodic **oscillatory** regime at finite integrated response, **F** is the unbounded, but ergodic **frozen** phase, **AF** the phase with **anomalous** response at $\alpha < \alpha_{c2} = 1/2$ and $\kappa > 0$ in which the system is **frozen**. Finally **AFO** marks the phase with **anomalous** response at $\kappa = 0, \alpha < \alpha_{c2} = 1/2$, in which both **frozen** and **oscillatory** solutions are found depending on initial conditions.

For the game with impact-correction ($\kappa > 0$) we could not find any oscillatory solutions below $\alpha = 1/2$ in numerical simulations. Independent of initial conditions, all observed states were fully frozen and unbounded in the sense of the above definitions, as indicated by non-zero values of λ_1 in Fig. 2, and showed a zero volatility for all $\alpha < 1/2$.

4. Phase diagram and discussion

The resulting phase diagram is depicted in Fig. 4, and we will now turn to a brief discussion of its main features, treating the two cases $\kappa = 0$ and $\kappa > 0$ separately:

4.1. $\kappa = 0$

For the game without impact-correction, we find three distinct phases: (i) an ergodic phase with **oscillatory** behaviour of the correlation function at $\alpha > \alpha_{c1} = 2$ (**O**), (ii) an unbounded **frozen** (but still ergodic) phase at intermediate $\alpha \in [1/2, 2]$ (**F**), and (iii) a phase with **anomalous** response below $\alpha = \alpha_{c2} = 1/2$, in which we can find both **oscillatory** and **frozen** states (**AFO**), depending on initial conditions (as illustrated in Fig. 1). Note also that the volatility displays a characteristic minimum at $\alpha = \alpha_c = 1/2$, very much like the fluctuations of the original MG (we find $\sigma^2(\alpha_c) = 0$, however, whereas the volatility in the conventional MG is always strictly positive at finite values of α). In contrast to the different spherical model discussed in [1] we find no discontinuities of the volatility or oscillation amplitude across any of the transitions.

4.2. $\kappa > 0$

The behaviour of the model with impact correction is qualitatively similar to the case $\kappa = 0$ for large values of α and as long as $\kappa \neq 1$. There we find an oscillatory phase at $\alpha > \alpha_{c1}(\kappa)$ separated from a frozen (but ergodic) phase at intermediate values of $1/2 < \alpha < \alpha_{c1}(\kappa)$. The critical value $\alpha_{c1}(\kappa)$ increases as κ is increased, with $\lim_{\kappa \rightarrow 1} \alpha_{c1}(\kappa) = \infty$, see Eq. (28), so that no oscillatory phase is found for the game with full impact-correction ($\kappa = 1$). Simulations confirm indeed that the game with full impact correction is in fully frozen state ($c_0 = 1$) for all α , see Fig. 2, in analogy with the conventional MG, where the same feature is observed at $\kappa = 1$ [8]. We note however, that the spherical model does not appear to exhibit a simultaneous onset of memory and replica symmetry breaking at finite susceptibility χ , as found in the conventional MG for $0 < \kappa < 1$ [9]. Instead we find that anomalous response ($\chi \rightarrow \infty$) sets in at $\alpha = 1/2$ irrespective of κ .

Below $\alpha = 1/2$ the system is hence in a state of anomalous response both for $\kappa = 0$ and for $\kappa > 0$. However, we do not observe any oscillatory states in simulations in this regime for $\kappa > 0$, while both oscillatory and frozen states are found below $\alpha = 1/2$ in the game without impact correction. In the above phase diagram we refer to the phase with anomalous response as **AF** for $\kappa > 0$, as opposed to **AFO** for $\kappa = 0$. In particular the volatility σ^2 turns out to vanish in this **AF** phase at $\kappa = 0$, whereas oscillatory high-volatility solutions can be found for $\kappa = 0, \alpha < 1/2$ and small initial bias. This results in a discontinuity of σ^2 at $\kappa = 0^+$ at any fixed value $\alpha < 1/2$ (and for sufficiently small initial bias), as shown in the upper panel of Fig. 5. We here plot σ^2 as a function of κ at fixed $\alpha = 0.1$ and find that $\sigma^2 = 0$ for all $\kappa > 0$, but that σ^2 is positive at $\kappa = 0$. The magnitude of this discontinuity depends on α and increases as $\alpha \rightarrow 0$ due to the increasing volatility in the oscillatory states of the game without impact-correction in this limit (Fig. 1). Note that the volatility is continuous at $\kappa = 0^+$ in the ergodic regime $\alpha > 1/2$, see the lower panel of Fig. 5. Again very similar behaviour has been found in the conventional MG and also in MGs with dilution [14, 11].

A further parallel to conventional MGs can be drawn upon noting that the normalization parameter $\lambda(t) = \lambda_0 + \lambda_1 t$ remains finite asymptotically ($\lambda_1 = 0$) for all $0 \leq \kappa < 1$ above $\alpha_{c1}(\kappa)$ but becomes divergent ($\lambda_1 > 0$) in the **F** phase at intermediate α . This reflects the behaviour of the fraction of frozen agents in the conventional MG (corresponding to runaway solutions) [6], which for $\kappa = 0$ is known to rise sharply as α is increased from the non-ergodic to the ergodic region. It decreases as α is increased further for conventional MGs at all $0 \leq \kappa < 1$ and vanishes in the limit $\alpha \rightarrow \infty$ [#]. In addition the fraction of frozen agents approaches unity as $\alpha \rightarrow 0$ for the conventional MG with impact correction ($\kappa > 0$), in analogy with the observed non-zero values for λ_1 in the **AF** phase of our model with $\kappa > 0$, see Fig. 2. The spherical model with full impact correction ($\kappa = 1$) has $\lambda_1 > 0$ for all α , its conventional counterpart is in a fully

[#] Note however that simulations of the game at $\kappa = 0$ in the **AFO** phase indicate that $\lambda_1 = 0$ even for high bias. In the conventional game one here finds a large fraction of frozen agents.

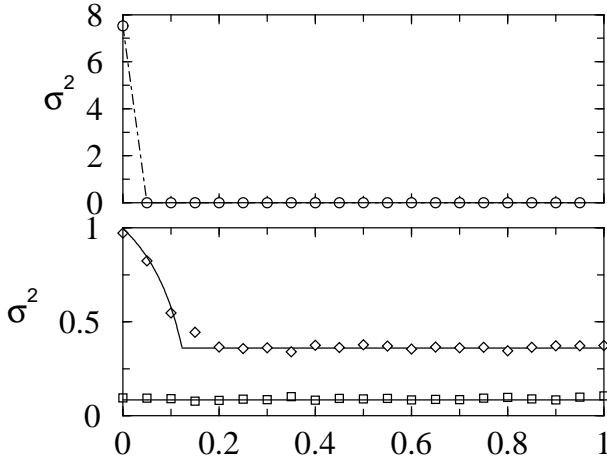


Figure 5. σ^2 vs κ for different values of α at initial bias $q_0 = 0.01$. Upper panel: $\alpha = 0.1$ (circles), where the system is in a non-ergodic state for all κ . Lower panel: $\alpha = 3.16$ (diamonds) and $\alpha = 1$ (squares). For $\alpha = 3.16$ the system is in the **F** phase above a critical value of $\kappa \approx 0.12$, and in an oscillatory state **O** below $\kappa \approx 0.12$. For $\alpha = 1$ the **F** is realised at all κ . Both panels: markers are from simulations, solid lines from theory for the respective phases. The dashed line in the upper panel is a guide to the eye.

frozen state irrespective of α .

5. Replica theory

We will now turn to the statics of the model. The starting point of the analysis of the statics of the standard MG without spherical constraints is the random function

$$H_\kappa(\boldsymbol{\varphi}) = \frac{1}{\alpha N} \sum_\mu \left(\sum_{i,j} \xi_i^\mu \xi_j^\mu \varphi_i \varphi_j + 2\sqrt{N} \sum_i \Omega^\mu \xi_i^\mu \varphi_i + N \Omega^\mu \Omega^\mu + \kappa \sum_i \xi_i^\mu \xi_i^\mu (1 - \varphi_i^2) \right). \quad (44)$$

The computation in the standard MG then proceeds by a minimization of H_κ in terms of the variables $\{\varphi_i\}$ using replica techniques. The $\{\varphi_i\}$ here correspond to temporal averages over the (discrete) spins $s_i(t) \in \{-1, 1\}$, i.e. one has $\varphi_i = \lim_{t \rightarrow \infty} t^{-1} \sum_{\tau \leq t} s_i(\tau)$ so that the $\{\varphi_i\}$ are continuous variables $-1 \leq \varphi_i \leq 1$. In the spherical model we have $\sum_i \phi_i(t)^2 = N$ at any given time t so that the temporal averages $\varphi_i = \lim_{t \rightarrow \infty} t^{-1} \sum_{\tau \leq t} \phi_i(\tau)$ are not individually constrained to the interval $[-1, 1]$, but fulfill a global constraint of the form $\sum_i \varphi_i^2 \leq N$. That is to say the vector $\boldsymbol{\varphi} = (\varphi_1, \dots, \varphi_N)$ can take values corresponding to any point *within* a sphere of radius \sqrt{N} , and is not constrained to its surface. Note that this inequality holds as an equality only if all $\{\phi_i(t)\}$ are time-independent, i.e. if a fully frozen state is reached. To capture cases different from this fully frozen state we first constrain $\boldsymbol{\varphi}$ to a shell of radius $r\sqrt{N}$, and will subsequently minimize the free energy with respect to $0 < r \leq 1$. We expect to

recover the frozen states as minima of H at $r = 1$, and will see below that minima at values $r < 1$ correspond to the oscillatory stationary states of the batch game.

At fixed r the replicated partition function at an ‘annealing temperature’ $T = \beta^{-1}$ is given by

$$(Z_r)^n = \int_{-\infty}^{\infty} \left[\prod_{ia} d\varphi_i^a \right] \left[\prod_a \delta \left(r^2 N - \sum_i (\varphi_i^a)^2 \right) \exp [-\beta H_\kappa(\varphi^a)] \right], \quad (45)$$

where we have introduced replicated fields $\{\varphi_i^a\}$. $a = 1, \dots, n$ is a replica index, and $\varphi^a = (\varphi_1^a, \dots, \varphi_N^a)$. The delta-functions in the above partition function enforce the spherical constraints on each of the sets $\{\varphi_i^a\}$, $a = 1, \dots, n$.

We will be interested in the limit $\beta \rightarrow \infty$ of the above expression eventually, as the minima of H_κ are found as

$$\lim_{N \rightarrow \infty} \min_{\{\varphi\}} \frac{H_\kappa(\varphi|r)}{N} = - \lim_{\beta \rightarrow \infty} \lim_{N \rightarrow \infty} \lim_{n \rightarrow 0} \frac{\overline{Z^n} - 1}{\beta N n}. \quad (46)$$

The notation $H_\kappa(\varphi|r)$ indicates that the fields are restricted to radius r at this stage. The computation of $\overline{(Z_r)^n}$ is lengthy but standard and follows the lines of [13, 11]. Upon making a replica symmetric ansatz one ends up with the following expression for the free energy given r

$$\begin{aligned} f_{r,RS}(Q, q, S, s, \rho) = & \frac{\alpha}{2\beta} \log \left[1 + \frac{\beta}{\alpha} (Q - q) \right] + \frac{\alpha}{2} \frac{(1+q)}{\alpha + \beta(Q-q)} \\ & + \frac{\alpha\beta}{2} (SQ - sq) - \frac{1}{\beta} \left\langle \log \int_{-\infty}^{\infty} d\varphi \exp (-\beta V_z(\varphi)) \right\rangle_z \\ & + \frac{\kappa}{2} (1 - Q) + \frac{1}{\beta} \rho (r^2 - Q), \end{aligned} \quad (47)$$

where Q and q are the diagonal and off-diagonal elements of the replica symmetric overlap matrix respectively, and S and s their conjugate variables. ρ is a Lagrange parameter enforcing the spherical constraint $Q = r^2$. $V_z(\varphi)$ is an effective potential defined by

$$V_z(\varphi) = -\sqrt{\alpha s} z \varphi - \frac{\alpha\beta}{2} (S - s) \varphi^2 \quad (48)$$

and $\langle \dots \rangle_z$ denotes an average over the standard Gaussian variable z .

The corresponding saddle-point equations are obtained by working out the variations of $f_{r,RS}$ with respect to the parameters $\{Q, q, S, s, \rho\}$. By construction, $\partial f_{r,RS} / \partial \rho = 0$ implies $Q = r^2$. The other saddle-point equations are found along the lines of [13, 11]. In the limit $\beta \rightarrow \infty$ we will be looking for solutions with $\lim_{\beta \rightarrow \infty} q = \lim_{\beta \rightarrow \infty} Q$ and $\lim_{\beta \rightarrow \infty} s = \lim_{\beta \rightarrow \infty} S$, and one defines the finite quantity $\chi = \lim_{\beta \rightarrow \infty} \frac{\beta}{\alpha} (Q - q)$. After some algebra the saddle-point equations lead to

$$\chi = [\sqrt{\alpha} \sqrt{1 + 1/r^2} - 1]^{-1}, \quad (49)$$

in direct correspondence to (27). The free energy at zero temperature reduces to

$$\begin{aligned} \lim_{\beta \rightarrow \infty} f_{r,RS} = & \frac{1}{2} \frac{1 + r^2}{(1 + \chi)^2} + \frac{\kappa}{2} (1 - r^2) \\ = & \frac{1}{2} \left[\sqrt{1 + r^2} - r/\sqrt{\alpha} \right]^2 + \frac{\kappa}{2} (1 - r^2). \end{aligned} \quad (50)$$

Finally we minimize this expression with respect to $0 < r \leq 1$. If the minimum is taken at $r = 1$ we expect the system to be fully frozen, while a minimum at $r < 1$ corresponds to an oscillatory state as found in the dynamics. For $\alpha > \alpha_{c1}$ (with α_{c1} as given in Eq. (28)) the absolute minimum of (50) in the interval $r \in [0, 1]$ is identified as

$$r^2 = \left[\frac{1 + (1 - \kappa)\alpha + \sqrt{[1 + (1 - \kappa)\alpha]^2 - 4\alpha}}{2\sqrt{\alpha}} - 1 \right]^{-1} < 1. \quad (51)$$

For $\alpha < \alpha_{c1}$ the minimum is attained at $r = 1$. Hence replica theory leads to the same expressions for the persistent order parameters as the generating functional analysis (see e.g. Eq. (26)), and in particular we find the same phase boundary between the **O** and **F** phases^{††}. Furthermore, the frozen phase ($r = 1$) obtained from the statics breaks down when $\chi \rightarrow \infty$, i.e. at $\alpha = \alpha_{c2} = 1/2$ (see Eq. (49)), again in agreement with the phase diagram obtained from the dynamics.

6. Continuous-time limit and general time-step

6.1. Continuous time

In this section we will consider a continuous time limit of our model. For simplicity we will restrict the discussion to the case without market impact correction, a generalization to non-zero values of κ is straightforward. We will thus consider

$$\frac{d}{dt}q_i(t) = -h_i - \sum_j J_{ij}\phi_j(t), \quad (52)$$

where $\phi_i(t) = q_i(t)/\lambda(t)$, with $\lambda(t) > 0$ chosen such that $\sum_{i=1}^N \phi_i^2(t) = N$ ⁺⁺. The effective single-agent process corresponding to (52) reads

$$\dot{q}(t) = -\alpha \int dt' (\mathbf{I} + G)^{-1}(t, t')\phi(t') + \theta(t) + \sqrt{\alpha}\eta(t) \quad (53)$$

(see also [15] for p -spin spherical spin glass models in continuous time). The order parameters C, G and λ are to be determined self-consistently according to

$$\langle \eta(t)\eta(t') \rangle_* = [(\mathbf{I} + G)^{-1}D(\mathbf{I} + G^T)^{-1}](t, t'), \quad (54)$$

$$C(t, t') = \langle \phi(t)\phi(t') \rangle_*, \quad G(t, t') = \frac{\delta}{\delta\theta(t')} \langle \phi(t) \rangle_*, \quad C(t, t) = 1. \quad (55)$$

Conversion into closed equations for the correlation and response functions gives

$$\begin{aligned} \frac{\partial}{\partial t} [\lambda(t)C(t, t')] &= -\alpha ((\mathbf{I} + G)^{-1}C)(t, t') \\ &\quad + \alpha ((\mathbf{I} + G)^{-1}D(\mathbf{I} + G^T)^{-1}G^T)(t, t'), \end{aligned} \quad (56)$$

^{††}Note that while the static approach allows one to distinguish between frozen phases ($c_0 = 1$) and phases which are not fully frozen ($c_0 < 1$), the shape of the correlation function cannot be determined from the replica analysis presented here. The referral to the latter phase as ‘oscillatory’ is therefore motivated by the previous analysis of the dynamics of the batch game

⁺⁺Note that this is similar but not identical to a Langevin equation $\dot{q}_i(t) = -\frac{\partial \mathcal{H}}{\partial q_i}$ with $\mathcal{H} = \frac{1}{2} \sum_{ij} J_{ij}q_i q_j + \sum_i h_i q_i$.

$$\frac{\partial}{\partial t} [\lambda(t)G(t, t')] = -\alpha ((\mathbf{1} + G)^{-1}G)(t, t') + \delta(t - t'). \quad (57)$$

Assuming that a time-translation invariant bounded state is reached, we may again write these equations in terms of the Fourier transforms of C and G , and find ($\lambda(t) \equiv \lambda_0$)

$$i\omega\lambda_0\tilde{C}(\omega) = -\alpha \frac{\tilde{C}(\omega)}{1 + \tilde{G}(\omega)} + \alpha \frac{\tilde{D}(\omega)\tilde{G}^*(\omega)}{|1 + \tilde{G}(\omega)|^2} \quad (58)$$

$$i\omega\lambda_0\tilde{G}(\omega) = -\alpha \frac{\tilde{G}(\omega)}{1 + \tilde{G}(\omega)} + 1 \quad (59)$$

Using $D(t - t') = 1 + C(t - t')$ and writing $\chi = \tilde{G}(0)$ as usual, we find that the equation for C gives

$$(i\omega|1 + \tilde{G}(\omega)|^2 + \alpha)C(\omega) = \alpha\chi 2\pi\delta(\omega). \quad (60)$$

Similarly to calculation in the spherical MG in discrete time, we conclude that $\tilde{C}(\omega)$ can be non-zero only for $\omega = 0$. In contrast to the model in discrete time, there are no oscillatory solutions. This does not seem to be surprising since the continuous-time dynamics of (52) can be expected to effectively correspond to a system with asynchronous random updating (as opposed to the parallel dynamics considered earlier) for which also in the conventional MG model global oscillations are suppressed [16]. While this correspondence to asynchronous updating in the MG still deserves further attention we note that synchronous updating in neural networks results in a description of the effective dynamics in terms of a discrete-time process, while asynchronous updating leads to equations in continuous time; see for example [17, 18] for further details.

It is easy to check that assuming a fully frozen state ($c_0 = 1$) in Eqs. (58) and (59) (evaluated at $\omega = 0$) implies $\alpha = 2$, so that we conclude that there can be no extended phase with bounded values of $\lambda(t)$ in the model in continuous time, neither a frozen nor an oscillatory one. It would then appear sensible to revert to our unbounded state $\lambda(t) = \lambda_0 + \lambda_1 t$, with $\lambda_1 > 0$ and to assume that $\phi(t)$ in the effective process approaches a fixed point (with value dependent on the realization of the single-particle noise). This then leads to Eq. (35) (where now $v = \lim_{t \rightarrow \infty} \dot{q}$), and hence to exactly the same solutions for χ and σ^2 as in the **F** phase of the game in discrete time. In particular one expects a breakdown of ergodicity at $\alpha = 1/2$ also for the model in continuous time.

6.2. Arbitrary, but finite time-step

One may ask whether this model in continuous time can be obtained as the limit $\delta \rightarrow 0$ of a model with time-step δ :

$$\frac{q_i(t + \delta) - q_i(t)}{\delta} = -h_i - \sum_j J_{ij}\phi_j(t). \quad (61)$$

δ can here also be understood as a learning rate, with which the agents process information and adjust their score updates and trading actions. We note that the left-hand side can be written as $[\lambda(t + \delta)\phi_i(t + \delta) - \lambda(t)\phi_i(t)]/\delta$ upon using $\phi_i(t) = q_i(t)/\lambda(t)$,

so that the only effect of the arbitrary time-step is a re-scaling of the $\{\lambda(t)\}$. Numerical simulations (not shown here) confirm that the oscillation amplitude of the correlation function $C(t-t') = \langle \phi(t)\phi(t') \rangle_*$ in the stationary state and the volatility are not affected by the introduction of a general time-step, but that the only effect is a rescaling of the $\{q_i(t)\}$ relative to the $\{\phi_i(t)\}$. This is at variance with the spherical model of [1], in which the phase diagram changes as the time-step (or equivalently the learning rate) is modified, as sketched in the appendix. Note that a subtle dependence of fluctuations on the learning rate has been observed in a different agent-based model with continuous degrees of freedom in [19, 20].

7. On-line game

Finally, it is interesting to compare the stationary states of the on-line model (defined by Eq. (7)) with those of the batch game. The persistent order parameters (such as c_0 and χ) are known to be identical in the stationary ergodic states of conventional batch and on-line MGs respectively [6], but differences in the volatility are in principle to be expected, as the latter depends not only on the persistent parts of the dynamical order parameters, but also explicitly on their transients. While these differences between batch and on-line games are negligible in conventional MGs with uncorrelated strategy assignments, crucial differences in their quantitative values and qualitative behaviour were reported for anti-correlated strategies in [16]. These differences can be attributed to persistent oscillatory behaviour of the batch game.

We compare results from numerical simulations of the batch and on-line games in Fig. 6. We restrict the discussion to the case without market impact correction here ($\kappa = 0$). As expected we observe an ergodic/non-ergodic transition at $\alpha = \alpha_{c2} = 1/2$ also in the on-line game and find that the persistent correlation c_0 of the on-line game takes the same values as that of the batch game in the ergodic regime. In particular $c_0 = 1$ in both games in the fully frozen state at intermediate α . Within the accuracy of the simulations the locations of the transitions are insensitive to the timing of adaptation (on-line versus batch) and in agreement with the batch theory.

The volatility σ^2 , however, shows a more intricate behaviour, see right panel of Fig. 6. While the volatilities of the two games agree perfectly in the frozen ergodic phase at intermediate $\alpha \in [1/2, 2]$ and are there given by Eq. (40), one finds differences between the batch and on-lines cases in the regime of high values of α , where the batch system oscillates in its stationary state. In this phase at $\alpha > 2$ the volatility of the batch game is given by Eq. (32), and contains contributions from the persistent as well as the oscillatory parts of the correlation and response functions. As shown in Fig. 6, the volatility of the on-line game is consistently smaller than that of the batch game in this regime. The spherical game presented here therefore presents another example of a MG in which the market fluctuations of the batch and on-line games differ from each other. As in [16] these differences can be attributed to the presence of persistent oscillations present in the batch game, but not in its on-line counterpart. Indeed, the

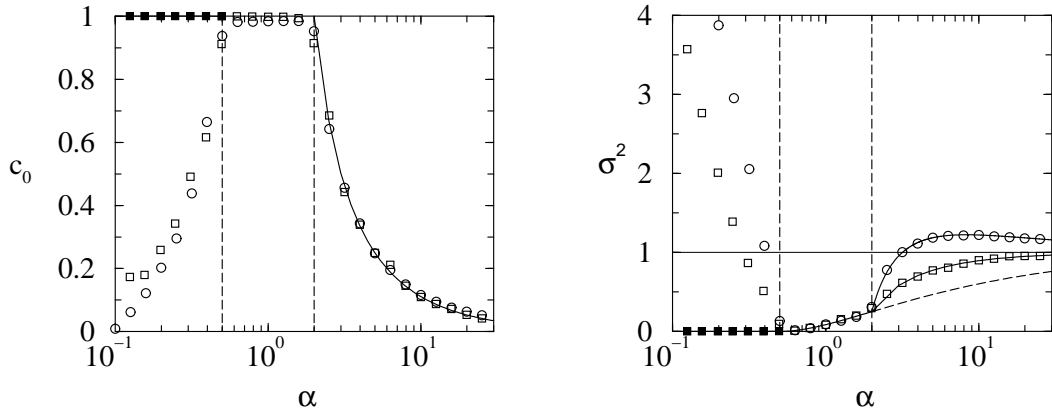


Figure 6. Persistent correlation c_0 and volatility σ^2 for the batch and on-line games without impact correction ($\kappa = 0$). Open circles are obtained from simulations of the batch game (simulation parameters as in the other figures), open squares correspond to the on-line game (simulations performed at $\alpha N^2 = 10^4$, run for 100000 on-line steps, 20 samples of the disorder). $q_0 = 0.01$ in both cases. Solid squares correspond to the on-line game with initial bias $q_0 = 3$. Solid lines are theoretical predictions, with the upper line for σ^2 in the high- α phase corresponding to the batch theory (Eq. (32)) and the lower solid line to the on-line approximation (62). The expression for the fully frozen phase has been continued into the high- α regime (where it is no longer valid neither for the on-line nor the batch game) as a dashed line.

volatility of the on-line game is consistently larger than the theoretical prediction one would obtain in a fully frozen state, see Fig. 6, and the now standard approximation

$$\sigma^2 = \frac{1}{2} \left[\frac{1 + c_0}{(1 + \chi)^2} + (1 - c_0) \right] \quad (62)$$

for the volatility in on-line games, obtained by suitably removing all non-persistent contributions to C and G (for details see [21, 6]) gives near perfect agreement with the numerical data. While (62) is at present only an approximate expression, an exact dynamical theory appears feasible for the present spherical game also with on-line dynamics (for example along the lines of [21]) and might allow one to derive an exact result for the volatility. Finally, we note that started from equal initial conditions the volatility of the on-line game is consistently smaller than that of the batch game also for $\alpha < 1/2$ (if the initial bias in this non-ergodic regime is small enough not to end up in a fully frozen regime, where $\sigma^2 = 0$ for both games). We recall that under these circumstances the stationary state of the batch game is again an oscillatory one.

8. Concluding remarks

In summary we have presented a detailed analysis of the stationary states of a spherical version of the MG, both from a static and a dynamical point of view. While the present model defines only a minor modification of an earlier spherical MG, we find that some of its features bear more similarity with those of the original MG. In particular one finds

a non-ergodic regime, characterized by a strong dependence of the stationary states on initial conditions, while the spherical model of [1] turned out to be ergodic for all values of the model parameters. Also the model presented here does not display any discontinuities in the volatility, but the characteristic minimum of σ^2 at the point at which the onset of non-ergodicity occurs. Despite this increased resemblance to the original MG, the model is still exactly solvable in the ergodic phases, and in particular exact expressions for the volatility can be obtained. The model also allows to study the dependence of volatilities on the timing of adaptation of the agents. Similar to [16] one finds that batch games in their oscillatory phases exhibit larger fluctuations of the total bid than an on-line game with the same model parameters. We are here able to give an exact expression for the batch volatility, and a very accurate approximation for the on-line case, whereas in [16] analytical results for the volatility of the batch game with fully anti-correlated strategies were restricted to upper and lower bounds. Hence, the present spherical model might serve as a starting point for a more detailed study of the differences between on-line and batch games, which are reminiscent of the ones recently observed for example in [18, 22] for sequential and synchronous updating in other spin systems. Two-cycles, i.e. persistent oscillations, play a crucial role in those studies similar to what is observed in our model and in the MG with anti-correlated strategies. A detailed analysis of an on-line version of the two spherical models might also help to elucidate the role of transients in the dynamics and the success of the *ad-hoc* removal of non-persistent parts of the correlation and response functions when deriving an approximate expression for the volatility. Finally, the dependence on initial conditions observed in the model discussed here might motivate further studies of its non-ergodic regime. Ideally, one would like to be able to compute the persistent order parameters as a function of the initial bias q_0 , which would most likely involve a detailed computation of the transient behaviour. One might hope that work along these lines could also help to shed some light on the non-ergodic, turbulent regime of the original MG, a thorough analytical understanding of which is still awaited.

Acknowledgements

This work was supported by the European Community's Human Potential Programme under contract HPRN-CT-2002-00319, STIPCO. TG acknowledges the award of a Rhodes Scholarship and support by Balliol College, Oxford. The authors would like to thank R Kühn and R Stinchcombe for discussions leading to the present work, as well as A C C Coolen for earlier collaborative work on spherical Minority Games.

References

- [1] Galla T, Coolen A C C, Sherrington D, *J.Phys A: Math. Gen.* **36** 11159
- [2] Berlin T H, Kac M 1952 *Physical Review* **86** 821
- [3] Bolle D, Nieuwenhuizen T M, Perez Castillo I, Verbeiren T 2003 *J. Phys. A* **36** 10269
- [4] Challet D and Zhang Y-C 1997 *Physica A* **246** 407

- [5] Challet D, Marsili M and Zhang Y-C 2005 *Minority Games* (Oxford University Press, Oxford UK)
- [6] Coolen ACC 2005 *The Mathematical Theory of Minority Games* (Oxford University Press, Oxford UK)
- [7] Johnson NF, Jefferies P and Hui PM 2003 *Financial market complexity* (Oxford University Press, Oxford UK)
- [8] De Martino A, Marsili M 2001 *J. Phys. A* **34** 2525
- [9] Heimel J A F, De Martino A 2001 *J. Phys. A: Math. Gen.* **34** L539
- [10] Heimel J A F and Coolen A C C 2001 *Phys. Rev. E* **63** 056121
- [11] Galla T 2005 *J. Stat. Mech.* P01002
- [12] Coolen A C C, Heimel J A F and Sherrington D 2001 *Phys. Rev. E* **65** 016126
- [13] Challet D, Marsili M and Zhang Y-C 2000 *Physica A* **276** 284
- [14] Marsili M, Challet D and Zecchina R 2000 *Physica A* **280** 522
- [15] Crisanti A, Horner H, Sommers H-J 1993 *Z. Phys. B* **92** 257
- [16] Galla T, Sherrington D 2005 *Eur. Phys. J. B* **46** 153
- [17] Coolen A C C 2001, in *Handbook of Biological Physics* Vol 4 (Elsevier Science, eds F Moss and S Gielen) 597, [cond-mat/0006011](https://arxiv.org/abs/cond-mat/0006011)
- [18] Bolle D, Busquets Blanco J 2004 [cond-mat/0408086](https://arxiv.org/abs/cond-mat/0408086)
- [19] Berg J, Marsili M, Rustichini A and Zecchina R 2001 *J. Quant. Finance* **1**(2) 203
- [20] De Martino A, Galla T 2005 *J. Stat. Mech.* 2005 P08008
- [21] Coolen A C C and Heimel J A F 2001 *J. Phys. A: Math. Gen.* **34** 10783
- [22] Bolle D, Busquets Blanco J 2005 [cond-mat/0505326](https://arxiv.org/abs/cond-mat/0505326)
- [23] Galla T 2004, D.Phil thesis, University of Oxford
- [24] Peretto P 1984, *Biol. Cybern.* **50** 51
- [25] Skantzos N S, Coolen A C C 2000 *J. Phys. A* **33** 5785

Appendix: Comparison of the two spherical models

In [1] a spherical limit of the dynamics of the MG was taken upon using the update rule

$$[1 + \lambda(t+1)]q_i(t+1) = q_i(t) - h_i - \sum_j J_{ij}q_j(t), \quad (63)$$

where the $\{\lambda(t)\}$ are chosen to impose a global spherical constraint $\sum_{i=1}^N q_i(t)^2 = Nr^2$. A perturbation field $\theta(t)$ may be added to the right-hand-side to generate response functions. The control parameters are given by α and r , and in order to be consistent with the spherical constraint initial conditions $\{q_i(t=0)\}$ were chosen such that $\sum_i q_i(0)^2 = Nr^2$. In this appendix we will first briefly summarise the main findings of [1] and then extend the analysis of [1] by studying the approach to its continuous-time limit and by a brief discussion of the statics of this earlier spherical model.

Phase diagram

Similar to the analysis in the main part of the paper the generating functional calculation in [1] leads to a coupled set of closed equations for the correlation and response functions (note that here one has $C_{tt'} = \lim_{N \rightarrow \infty} N^{-1} \sum_i \overline{\langle q_i(t)q_i(t') \rangle}$ and $G_{tt'} = \lim_{N \rightarrow \infty} N^{-1} \sum_i \partial \overline{\langle q_i(t) \rangle} / \partial \theta(t')$):

$$\begin{aligned} [1 + \lambda(t+1)]C_{t+1,t'} &= C_{tt'} + \alpha[(\mathbf{I} + G)^{-1}D(\mathbf{I} + G^T)^{-1}G^T]_{tt'} \\ &\quad - \alpha[(\mathbf{I} + G)^{-1}C]_{tt'}, \end{aligned} \quad (64)$$

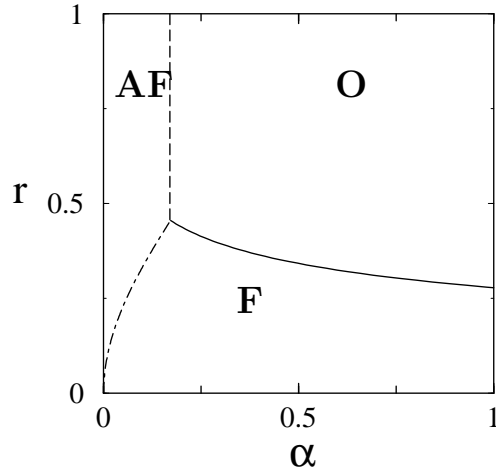


Figure 7. Phase diagram of the spherical MG studied in [1], displaying three phases: **O**, oscillating correlation function and finite integrated response; **F**, frozen phase with finite integrated response; and **AF**, anomalous frozen phase with diverging integrated response. Throughout the phase AF the volatility is zero. The $O \leftrightarrow F$ transition and the $F \leftrightarrow AF$ transition are continuous. The discontinuous transition from $O \leftrightarrow AF$ occurs at $\alpha = 3 - 2\sqrt{2} \approx 0.172$. The triple point corresponds to $\alpha = 3 - 2\sqrt{2}$ and $r = r^* \approx 0.455$. The dotted-dashed line separating the two frozen phases is given by $\alpha = r^2/(1 + r^2)$.

$$[1 + \lambda(t + 1)] G_{t+1, t'} = G_{tt'} - \alpha[(\mathbf{1} + G)^{-1} G]_{tt'} + \delta_{tt'}, \quad (65)$$

from which the stationary states of the model can be computed in a very similar way to the analysis in the main text of this paper. The resulting phase diagram is depicted in Fig. 7, and displays three distinct phases **O**, **F** and **AF**, similar to the model studied in this paper. All phases are bounded however, as runaway solutions $|q_i(t)| \rightarrow \infty$ are impeded by the spherical constraint on the $\{q_i\}$. While the transitions $O \leftrightarrow F$ and $F \leftrightarrow AF$ are continuous, a jump occurs in the volatility and oscillation amplitude across the $O \leftrightarrow AF$ transition. In particular one finds that the volatility vanishes identically throughout the **AF** phase, where $\chi = \infty$. The macroscopic order parameters (including σ^2) show no dependence on initial conditions in any part of the phase diagram, in contrast to the model devised in this paper**.

**Note that in [1] the second moment of the distribution of initial conditions was fixed by $N^{-1} \sum_i q_i(0)^2 = r^2$ for consistency as this normalization on the $\{q_i(t)\}$ is imposed for all subsequent times. The freedom of choosing initial conditions in [1] was thus limited to distributions with this fixed value of their second moment which in turn plays the role of a model parameter. In the present model no constraint on the $\{q_i(t)\}$ applies so that initial conditions $\{q_i(t=0)\}$ can be chosen arbitrarily. The analysis in the main part of the paper shows that different second moments $\lambda(0)^2 = N^{-1} \sum_i q_i(0)^2$ lead to different macroscopic stationary states for $\alpha < 1/2$.

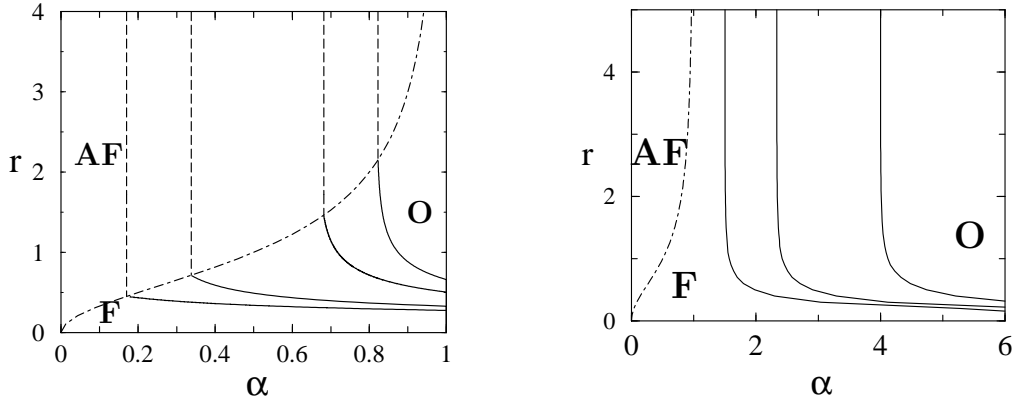


Figure 8. Phase diagram of the model of [1] for general time-step δ . Left ($\delta > 1/2$): solid lines: continuous $O \leftrightarrow F$ transition for $\delta = 1.0, 0.8, 0.6, 0.55$ (from left to right). The dotted-dashed line is given by $\alpha = r^2/(1+r^2)$ and marks the $F \leftrightarrow AF$ transition. Right: phase diagram for $\delta < 1/2$: solid lines: continuous $O \leftrightarrow F$ transition for $\delta = 0.4, 0.3, 0.2$ (from left to right). The dotted-dashed line is given by $\alpha = r^2/(1+r^2)$ and marks the $F \leftrightarrow AF$ transition.

Approach of the continuous-time limit

The model defined by (63) is easily generalised to arbitrary (but finite) values δ of the batch time-step:

$$\frac{[1 + \lambda(t + \delta)]q_i(t + \delta) - q_i(t)}{\delta} = -h_i - \sum_j J_{ij} q_j(t), \quad (66)$$

$$\frac{1}{N} \sum_i q_i^2(t) = r^2 \quad \text{for all } t, \quad (67)$$

and the analysis of the stationary states is easily adapted accordingly. In contrast to the model discussed in the main part of the paper, one here observes interesting effects on the phase diagram. For $1/2 < \delta < 2$ we find that the phase diagram and types of transitions are essentially preserved, but that the triple point moves according to $\alpha = (\sqrt{2/\delta} - 1)^2$ along the line $\alpha(r) = r^2/(1+r^2)$ as δ is varied, and that the numerical values of the locations of the different transitions change accordingly, as depicted in the left panel of Fig. 8. In the case of small $\delta < 1/2$ the discontinuous $O \leftrightarrow AF$ transition is no longer present, and the range of the oscillatory phase moves towards large values of α and r as δ is decreased, see the right panel of Fig. 8. In the limit $\delta \rightarrow 0$ the oscillatory phase will eventually no longer be present, so that the resulting model in continuous time only displays the **F** and **AF** phases, respectively, separated by a continuous transition at $\alpha = r^2/(1+r^2)$. As before all order parameters can be computed exactly for arbitrary values of δ in all phases, and numerical simulations (not shown here) confirm these results as well as the changes in the phase diagram [23].

Statics Finally, we note that the statics of the model (63) can be studied upon minimizing the Hamiltonian $H_{\kappa=0}$ defined in (44) [23]. Again the variables $\{\varphi_i\}$ are to be constrained to a sphere of radius r , where now r is a model parameter and

fixed (i.e. the free energy is not minimized with respect to r). Indeed the dynamical approach via generating functionals and the static calculation via replica methods turn out to deliver the same order parameters in the **F** phase of the model defined by (63). However, a replica approach along the lines of the main part of this paper (in which ground state solutions are not constrained to the surface of the sphere with radius r but can lie anywhere within) fails to reproduce the dynamical results obtained for the oscillatory regime of (63). It appears that here a more sophisticated approach based on (pseudo-) Hamiltonians of the Peretto type [24, 25] might be required, possibly along the lines of [18, 22].